

Disparate Impact of Osteocyte Oxygen-Sensing Mechanisms on Bone Quality

Kristina V. Wells¹, Sarah V. Mendoza¹, Alice Wong¹, Nicholas Hum², Aimy Sebastian², Deepa K. Muruges², Gabriela G. Loots^{1,2}, Clare E. Yellowley¹, Damian C. Genetos¹

¹University of California, Davis, Davis CA, ²Lawrence Livermore National Laboratory
kvwells@ucdavis.edu

Disclosures: The authors have no disclosures.

INTRODUCTION: Bone strength involves bone quantity and quality, with bone quantity receiving greater engagement and investigation than bone quality. Ideal osteoanabolic therapies should improve both the quantity and the quality of bone matrix. We have recently demonstrated that constitutive osteocytic oxygen sensing (degradation resistant *HIF-2α*, *HIF-2α* cDR) or a regulatory protein upstream of oxygen sensing (*Vhl* cKO) produce unique high bone mass phenotypes¹. While both disruptions increase cortical and trabecular bone, *HIF-2α* cDR does not phenocopy *Vhl* cKO either in quantity of bone produced or apparent bone organization. Despite both producing high bone mass phenotypes, data from our lab shows that *Vhl* cKO and *HIF-2α* cDR display marked differences in strength. Three-point bending test revealed that *Vhl* cKO mice have a higher ultimate force and stiffness, yielding stronger bones than wildtype; *HIF-2α* cDR is weaker than wildtype represented by lower stiffness, lower ultimate force, and higher post yield displacement. Understanding overlapping and unique contributions to bone quality in *Vhl* cKO vs. *HIF-2α* cDR will identify ideal targets for osteoanabolic therapies.

METHODS: We developed mice according to our approved IACUC with osteocyte-enriched (10kb-*Dmp1*-cre) deletion of the oxygen-sensitive transcription factors *Hif1a* or *Hif2a*, the E3 ubiquitin ligase (*Vhl*) responsible for HIF degradation, or mice with degradation-resistant (cDR) isoforms of *HIF-1α* or *HIF-2α*. Female mice were humanely euthanized at 16 weeks of age and femora were isolated for microcomputed tomography-based assessment of mineralization parameters. Tissue mineral density distribution (TMDD) within mid-diaphyseal cortical bone was obtained by distributing voxels into 100 evenly-spaced bins (400-1500 mg HA/cm³) to determine mean calcium content (Ca_{MEAN}), peak calcium content (Ca_{PEAK}), and width at half-maximum (Ca_{WIDTH}). Collagen alignment across genotypes was visualized by second harmonic generation (SHG) imaging of unstained 5μm thick femur sections. Collagen alignment, width and length were analyzed by ImageJ and CTFIRE software. Mineralization and collagen alignment were compared using one-way ANOVA and Tukey's post-hoc test. Bulk RNA-seq analysis was performed with DESeq2² to identify potential molecular mechanisms driving differences in bone quality; false discovery rate adjusted p-value <0.05 and fold change >1.5 were considered significantly differentially expressed.

RESULTS: Because we have previously found marked differences in biomechanical strength in two unique high bone mass models of disrupted osteocytic oxygen sensing, we chose to elaborate the impact on bone material properties in these models. TMDD quantitates the spatial distribution of mineral concentration which provides insight into the material properties of bone. Both *Vhl* cKO (n=3) and *HIF-2α* cDR (n=5) mice display reduced mid-cortical Ca_{PEAK} (*Vhl* cKO: 1056 vs 1182 mg HA/cm³, p<0.001; *HIF-2α* cDR: 1067 vs 1182 mg HA/cm³, p<0.001) and Ca_{MEAN} (*Vhl* cKO: 958 vs 1119 mg HA/cm³, p<0.001; *HIF-2α* cDR: 937 vs 1119 mg HA/cm³, p<0.001) relative to wildtype (n=7) littermate controls (**Figure 1A**) indicating impaired tissue material properties despite similar impact on structural properties. Heatmaps of mineral distribution reveal that the areas of low mineralization coincide with areas of dystrophic bone on the endocortical surface in both *Vhl* cKO and *HIF-2α* cDR (**Figure 1B**). Because mineralization was altered, we next investigated collagen orientation as another material property. SHG imaging of both *Vhl* cKO and *HIF-2α* cDR revealed the existence of both morphologically normal and abnormal bone in the cortical mid-diaphysis, which was reflected in analysis of SHG images. Both *Vhl* cKO and *HIF-2α* cDR displayed a cortical shell comprised of lamellar bone. An extension of the cortical bone on the endosteal surface was dystrophic, containing no clear lamellae and many open marrow spaces (**Figure 2**). Collagen alignment and distribution in lamellar cortical bone was not different across genotypes; in contrast, dystrophic endosteal cortical bone was more disorganized in *HIF-2α* cDR compared to wildtype. Image analysis demonstrated that only dystrophic bone in *HIF-2α* cDR had a higher mean deviation (24.3 vs 9.4, p=0.008) and lower alignment index of the collagen (0.46 vs 0.79, p=0.008) with concomitant thicker collagen fibers (5.7 vs 5.1 pixels, p=0.001) relative to wildtype. Bulk RNAseq of wildtype and mutant femora demonstrated disparate expression of lysyl oxidase isoforms as well as matrix metalloproteinases involved in collagen processing and reorganization in response to load in *HIF-2α* cDR mice (**Figure 3**).

DISCUSSION: *Vhl* cKO and *HIF-2α* cDR mice both demonstrate reduced mineralization, suggesting that constitutive HIF2α expression may promote increased deposition of poorly mineralized bone. However, *Vhl* cKO and *HIF-2α* cDR are not identical in bone quality, as only *HIF-2α* cDR displays alterations in collagen organization. This suggests that HIF-independent targets of *Vhl* may act in a compensatory manner to rescue collagen processing in *Vhl* cKO mice. One such target of this HIF-independent signaling may be lysyl oxidase, which was reduced only in *HIF-2α* cDR mice relative to wildtype.

SIGNIFICANCE: Our data suggests that both HIF-dependent and HIF-independent targets of *Vhl* impact bone quality. Identifying HIF-independent targets of *Vhl* may reveal novel therapies which promote osteoanabolism without sacrificing bone quality.

REFERENCES: 1. PMID: 37065633 2. PMID: 25516281

ACKNOWLEDGEMENTS: This work was supported by the National Institute of Arthritis and Musculoskeletal and Skin Diseases of the National Institutes of Health under award number 5-R01 AR073772-02 (CEY, DCG). DKM, NH, AS and GGL performed work under the auspices of the USDOE by LLNL (DE-AC52-07NA27344).

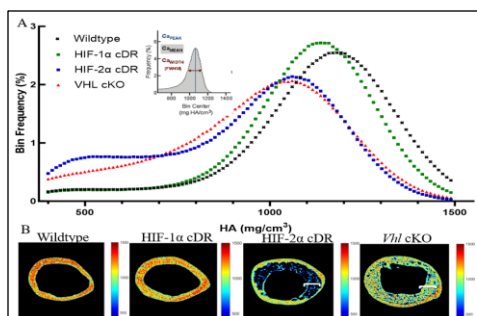


Figure 1: *Vhl* cKO and *HIF-2α* cDR produce less mineralized bone. (A) *Vhl* cKO and *HIF-2α* cDR have lower Ca_{PEAK} and Ca_{MEAN} compared to wildtype. (B) Less mineralized bone is localized to dystrophic bone (white bracket).

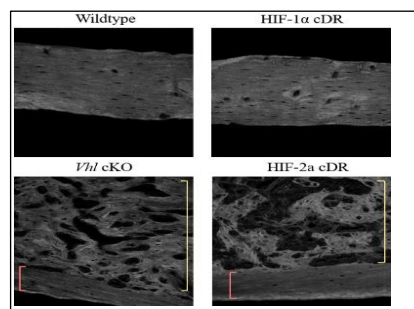


Figure 2: *Vhl* cKO and *HIF-2α* cDR produce more disorganized bone. *Vhl* cKO and *HIF-2α* cDR both produce dystrophic bone (yellow bracket) at the endosteal surface while both maintain lamellar cortical shell (red bracket).

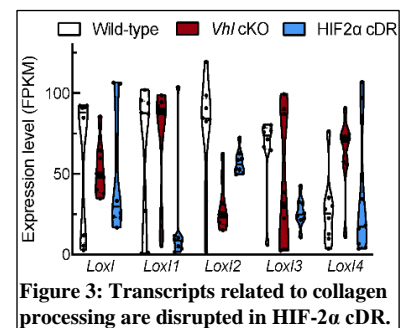


Figure 3: Transcripts related to collagen processing are disrupted in *HIF-2α* cDR.